Revista Brasileira de Geofísica
RBGf
Brazilian Journal of Geophysics

Revista Brasileira de Geofísica (2012) 30(4): 505-518
© 2012 Sociedade Brasileira de Geofísica
ISSN 0102-261X
www.scielo.br/rbg

CHANGE DETECTION SOFTWARE USING SELF-ORGANIZING FEATURE MAPS

Nilton Correia da Silva[1], Osmar Abílio de Carvalho Júnior[2],
Antonio Nuno de Castro Santa Rosa[3], Renato Fontes Guimarães[2]
and Roberto Arnaldo Trancoso Gomes[2]

Recebido em 6 junho, 2011 / Aceito em 7 maio, 2012
Received on June 6, 2011 / Accepted on May 7, 2012

ABSTRACT. Self-organizing feature maps (SOFM) consist of a type of artificial neural network that allows the conversion from high-dimensional data into simple geometric relationships with low-dimensionality. This method can also be used for classification of remote sensing images because it allows the compression of high-dimensional data while preserving the most important topological and metric relationships of the primary data. This paper aims to develop an effective methodology for using self-organizing maps in change detection. In this study, SOFM is used for unsupervised classification of remote sensing data, considering the following attributes: spatial (x and y), spectral and temporal. The method is tested and simulated in the western region of Bahia that has observed a significant increase in mechanized agriculture. Tests were performed with the SOFM parameters for the purpose of fine tuning a change detection map. The SOFM provides the best selection of cell and corresponding adjustment of weight vectors, which show the process of ordering and hierarchical clustering of the data. This information is essential to identify changes over time. All algorithms were implemented in C++ language.

Keywords: unsupervised classification, land cover, multitemporal analysis, remote sensing.

RESUMO. Os mapas auto-organizáveis (SOFM) consistem em um tipo de rede neural artificial que permite a conversão de dados de alta dimensão, complexos e não lineares, em simples relações geométricas com baixa dimensionalidade. Este método também pode ser utilizado para a classificação de imagens de sensoriamento remoto, pois permite a compressão de dados de alta dimensão preservando as relações topológicas dos dados primários. Este trabalho objetiva desenvolver uma metodologia eficaz para a utilização de mapas auto-organizáveis na detecção de mudanças. No presente estudo o SOFM é utilizado para a classificação não supervisionada de dados de sensoriamento remoto, considerando os seguintes atributos: espaciais (x, y), espectrais e temporais. O método é empregado na região oeste da Bahia, que teve recentemente um aumento significativo em monoculturas. Testes foram realizados com os parâmetros do SOFM com o objetivo de refinar o mapa de detecção de mudanças. O SOFM possibilita uma melhor seleção de células e dos correspondentes vetores de peso, que mostram o processo de ordenação e agrupamento hierárquico dos dados. Esta informação é essencial para identificar mudanças ao longo do tempo. Um programa em linguagem C ++ do método proposto foi desenvolvido.

Palavras-chave: classificação não supervisionada, cobertura da terra, análise multitemporal, sensoriamento remoto.

[1]Faculdade de Engenharias do Gama, Universidade de Brasília, Campus Gama, 72444-240 Brasília, DF, Brazil – Email: niltoncs@unb.br

[2]Universidade de Brasília, Departamento de Geografia, Campus Universitário Darcy Ribeiro, Asa Norte, 70910-900 Brasília, DF, Brazil. Phone: +55(61) 3071-859; Fax: +55(61) 2721-909 – E-mails: osmarjr@unb.br; renatofg@unb.br; robertogomes@unb.br

[3]Universidade de Brasília (UnB), Instituto de Geociências, Campus Universitário Darcy Ribeiro, Asa Norte, 70910-900 Brasília, DF, Brazil. Phone/Fax: +55(61) 3273-4735 – E-mail: nunos@unb.br

INTRODUCTION

Change detection is a process of identifying differences in the state of the object or phenomenon on different dates (Singh, 1989). Two types of temporal image processing stand out (Lambin, 1999): (a) discrete model – analysis of change detection based in bi-temporal images, and (b) continuous model – analysis of a dense temporal series to allow a description of the trajectory of surface dynamic and evolution, such as, for instance, the phenological behavior of the plant or the flooding of rivers.

This work is restricted to analysis of change on the basis of bi-temporal data, discrete over time. One advantage of the discrete model is that it allows a simple and fast description of the spatial dynamics. Many works propose a classification of the techniques of change detection using bi-temporal images (Singh, 1989; Lambin, 1999; Hall & Hay, 2003; Lu et al., 2003; Coppin et al., 2004). Normally, these methods are subdivided into two types: pre-classification and post-classification (Jensen et al., 1993, Yuan et al., 2005).

The pre-classification methods involve, firstly, the joint processing of the temporal images, so as to generate a new, unclassified image in which the features of the change are enhanced (Yuan & Elvidge, 1998). Among the types of processing used in change detection based on temporal images, the following stand out: algebraic operations, principally subtraction and division (Coppin et al., 2001; Dymond et al., 2002; Franklin et al., 2000, 2002, 2003; Gong et al., 1992; Skakun et al., 2003), linear transformations (Byrne et al., 1980; Fung & LeDrew, 1987; Cakir et al., 2006) and spectral measurements (Carvalho Júnior et al., 2011). One problem in this enhancing technique is classifying the areas of change after enhancement. Normally this is done by determining threshold values to delimit the areas of change or no change.

In the post-classification method every image is previously classified individually and then compared, extracting and quantifying the areas of change (Howarth & Wickware, 1981). Classification may be done manually or automatically using a supervised or unsupervised classifier. As described by Menke et al. (2009) the advantages of using this procedure are: (a) ease of updating over time, favoring monitoring; (b) allows to compensate the variations resulting from atmospheric conditions, phenological changes and soil humidity, due to independence in the generation of the thematic map; and (c) allows the integration and comparison of images from sensors with different spatial, spectral, temporal and radiometric resolutions, (d) allows the detection of categories of change, not limited to detecting only the classes of changes and no changes. As disadvantages, Menke et al. (2009) describe the following factors: (a) it is not fully automatic, making it a slower process; and (b) the accuracy to detect the changes depends on the accuracy of classification in each time, which may facilitate the propagation of errors. One form of automating the post-classification procedure is to use unsupervised classifiers. However, the use of unsupervised classifier independently for each image will be unlikely to present parameters describing the same class at two exactly-equal times. This may led to losses and errors in cross-checking the information between the two discrete times.

Another approach to detect changes would be to perform the automatic classification directly on the temporal images, denominated by Singh (1989) as "Direct Multidate Classification". This procedure has a different approach in relation to the two methods already described (post-classification and pre-classification), and may be denominated as syn-classification, since the classification and temporal processing are carried out together. This procedure avoids the errors contained in a classification performed independently for the two times, particularly when automatic methods are used. The unsupervised classifiers mostly used in change detection are those based on group analysis (Weismiller et al., 1977; Soares & Hoffer, 1994) or artificial neural networks (Dai & Korram, 1999; Nemmour & Chibani, 2005). Some authors, rather than adopting directly the spectral bands as input data for classification make use of previously treated images such as vegetation indices or components of the Tasseled Cap (Hayes & Sader, 2001; Sader et al., 2001; Wilson & Sader, 2002; Jin & Sade, 2005).

The aim of this article is to develop a method of unsupervised change detection based on the SOFM algorithm (SOFM - acronym for Self-Organizing Feature Maps), which consists of those most used in an Artificial Neural Network (ANN) to reduce the dimensionality of the data. The employment of SOFM as an unsupervised learning algorithm in remote sensing experiences intense development and has evidenced significant results (Gopal & Woodcock, 1996; Carpenter et al., 1997; 1999; Gopal et al., 1999; Jianwen & Bagan, 2005; Papa et al., 2010). The existing methods of change detection using the ANN consider the image from time 2 (t_2) as a spectral extension of the image from time 1 (t_1) (Dai & Korram, 1999; Nemmour & Chibani, 2005). However, this alternative prevents the obtainment of classified images for each time, which would help in the assessment and adjustment of the classification parameters. This work proposes a new configuration of the input data, generated after trainning the network based on two temporal images, and generates an independent classification for each time. A program of the method proposed has been developed in C++ language.

The proposed method is tested in an area of agricultural expansion in the West of Bahia State which has displayed a high spatial dynamic since the 1990's, with the advance of mechanized agriculture over the vegetation of the Cerrado grasslands. The region displays favorable conditions for the spread of agribusiness, such as: flat land, high insolation rates, high precipitation (1600 mm/year), concentrated between the months of October and March, besides government incentive (Smith et al., 1998; Kaimowitz & Smith, 2001).

METHODOLOGY

Theoretical review of Self-Organizing Feature Maps (SOFM)

Self-Organizing Feature Maps are known as an unsupervised competitive learning system capable of extracting characteristics from a set of training data. Based on a two-dimensional layer of neurons, represented by a set of initial weights, the SOFM training algorithm performs a self-organization of these neurons, so that they start to represent the characteristics of the training set used (Kohonen & Mäkisara, 1989; Kohonen 1982; 1988; 1990). Therefore, the challenge of learning in self-organizing maps is to cause, in different parts of the network, significant correlations for certain patterns of input.

The SOFM considers in the learning process, topological information on the space present in the input data in a competitive process. In the case of a training set consisting of pixels of images (spectra), at the end of the training, the set of neurons will characterize spectral classes (Silva, 2003).

The laws of competitive learning have as a common property a process of competition involving some or all of the neurons from the neural network, which always happens before each learning episode. The neurons that come out as winners in the competition have their weights updated (or have their weights updated in a manner differentiated from the other, non-winning, neurons). Even though the law of learning was introduced by various authors (Grossberg, 1976; Tsypkin, 1973; Williams, 1985), Kohonen was the first to focus clearly on the characteristic of equi-probability. The basic idea of Kohonen's learning algorithm is to select a layer of neurons whose weights have a distribution in space R^n, according to the input vectors "$\mathbf{e}$" used in the training of this layer (Hecht-Nielsen, 1990).

The SOFM consists of two layers, a single-dimension input layer and a two-dimensional grid layer with an arbitrary number of units (Kohonen, 1990). Each unit of the input layer is connected to all the units in the layer related to the grid. Figure 1 shows the basic structure of the *Kohonen layer* which consists of K neurons, each one receiving n signals $e_1, e_2, \ldots, e_n$ from the input layer. Input e_j for Kohonen neuron i has a real weight m_{ij} associated to it. The residual between the input and each neuron is calculated according to:

$$D(\mathbf{m}_i, \mathbf{e}), \tag{1}$$

In which, $\mathbf{m}_i = (m_{i1}, m_{i2}, \ldots, m_{in})^T$, $\mathbf{e} = (e_1, e_2, \ldots, e_n)^T$ and $D(\mathbf{m}_i, \mathbf{e})$ is the function of measurement of distance (which need not necessarily be a metric distance). Two more common types for $D(\mathbf{m}_i, \mathbf{e})$ are the Euclidean distance ($D(\mathbf{m}_i, \mathbf{e}) = |\mathbf{m}_i - \mathbf{e}|$) and the distance of the spherical arc ($s(\mathbf{m}_i, \mathbf{e}) = 1 - \mathbf{m}_i \cdot \mathbf{e} = 1 - \cos\phi$; where $\mathbf{m}_i$ and $\mathbf{e}$ are vectors of unit size and ϕ the angle between them).

The competition among the neurons assessthe intensity of entry of the neurons, in other words, the neuron with $\mathbf{m}$ weights, closest to $\mathbf{e}$. To demonstrate how Kohonen learning takes place, consider a two-dimensional matrix of units of neurons disposed in a hexagonal layer (Fig. 1). For each neuron (or node) i of this layer, one weight vector is linked, varying with time $\mathbf{m}_i(t) \in R^n$, $t = 0, 1, 2, \ldots$. The $\mathbf{m}_i(0)$ may be random. Assume that an input pattern vector $\mathbf{e}(t) \in R^n$ is received and compared to each weight vector $\mathbf{m}_i(t)$. Two rules define how the mapping of patterns is formed by self-organization when a sufficient number of input vectors is received by the network. The first rule is to find the unit c whose weight vector $\mathbf{m}_i(t)$ bears the greatest similarity with $\mathbf{e}(t)$:

$$\left\|\mathbf{e}(t) - \mathbf{m}_c(t)\right\| = \min_i \left\{\left\|\mathbf{e}(t) - \mathbf{m}_i(t)\right\|\right\} \tag{2}$$

Unit c is considered as the unit that responds to $\mathbf{e}(t)$. In the simplest case the Euclidean distance is used.

The second rule consists of modifying the weight vectors of unit c and its topological neighbors (Fig. 2). The topological neighborhood N_c refers to a subset of the layer of neurons close to the winning neuron and quite often it is a function dependent on the training cycle ($N_c(t)$).

The law of adaptation of this model takes the following criterion:

$$\left.\begin{array}{l} \mathbf{m}_i(t+1) = \mathbf{m}_i(t) + \alpha(t)[\mathbf{e}(t) - \mathbf{m}_i(t)],\ i \in N_c \\ \mathbf{m}_i(t+1) = \mathbf{m}_i(t),\ i \notin N_c \end{array}\right\} \tag{3}$$

In which, $a(t)$ is a scale that represents the intensity of gain of adaptation of the winning neuron. This parameter has a smooth decrease depending on the training cycle during the network's learning process ($a < a(t) < 1$). The radius of N_c decreases linearly during the training period (Kohonen & Mäkisara, 1989).

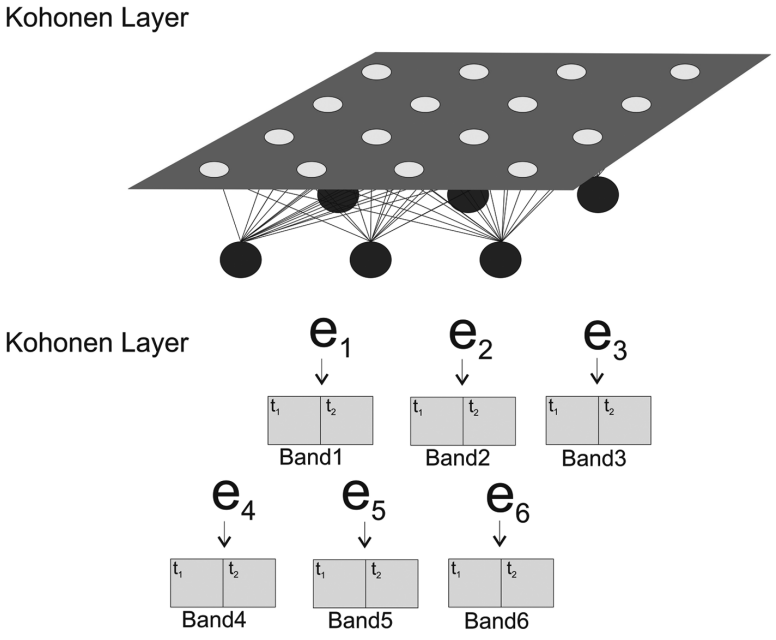

Figure 1 – The N neurons of the Kohonen layer receive, each one, n inputs $e_1, e_2 \ldots, e_n$. Each input has a weight m_{ij} associated to it. When each vector $\mathbf{e}$ is presented to the Kohonen layer, the neurons compete with one another, evidencing which weight vector $\mathbf{m}_i (\mathbf{m}_i = (m_{i1}, m_{i2}, \ldots, m_{in})$ is closest to $\mathbf{e}$.

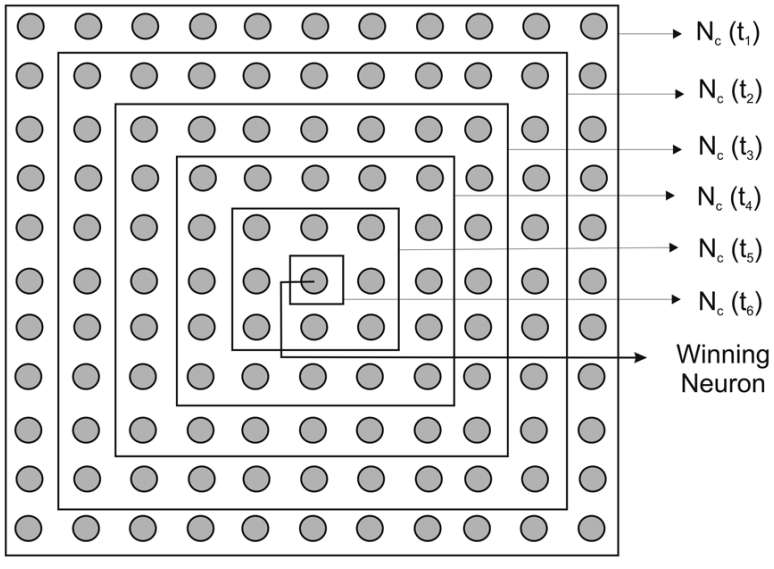

Figure 2 – The winning neuron and its topological neighborhood. Neighborhood function $N_c(t_i)$ defines the subset of neurons that will have their weights updated according to equation 3.

Pre-processing of temporal images

The choice of images normally considers acquisition dates at the same season of the year, seeking to minimize seasonal effects resulting from the phenology of the plants and climatic conditions (rain and humidity) (Lu et al., 2003). This study makes use of TM-Landsat images referring to the dates of June 20, 1984 and June 17, 2006 (Fig. 3).

The images must be co-registered to ensure a suitable georeferencing, so as not to generate detections of false changes as a result of a mere displacement between the temporal images. In this work the images are co-registered using the program

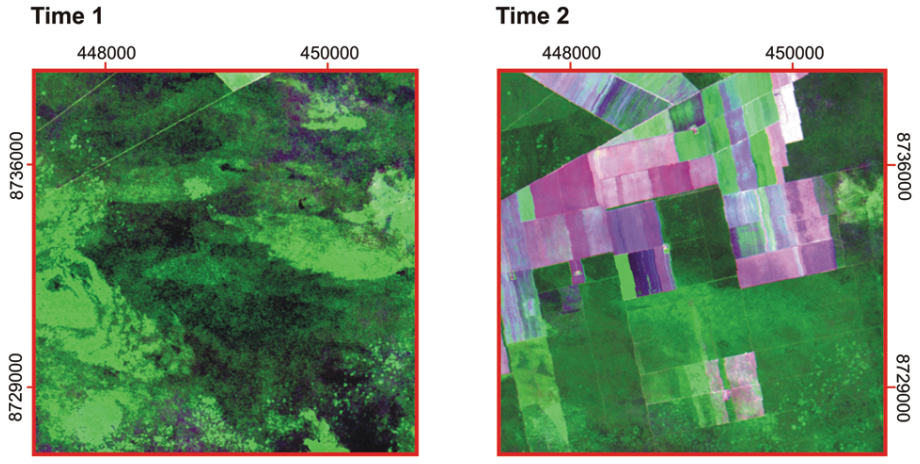

Figure 3 – Bi-temporal images of the study area referring to time 1 (Jun. 20 1984) and time 2 (Jun. 17 2006).

Environment for Visualizing Images – ENVI (Research Systems, 2001), maintaining the same dimensions of lines and columns. The mean squared error values prove to be below 0.2 pixels, which, according to Dai & Khorram (1998) eliminates the presence of features of anomalous change arising from lack of spatial correspondence.

The images must also be submitted to a radiometric normalization, to ensure homogeneous spectral responses from the targets at the different times under analysis. A first correction may be made based on conversion of the gray levels for apparent reflectance, which normalizes the following effects: illumination, solar irradiance at the top of the atmosphere and the angle of incidence of radiation on the target (Ponzoni & Shimabukuro, 2007). However, even after conversion to reflectance, some differences may still remain, arising mainly from atmospheric effects. In this condition, two alternatives for correction are proposed: (a) absolute atmospheric correction, which adopts codes of radioactive transfer, or (b) relative atmospheric correction, where the data from an image are adjusted to a reference image (known as radiometric calibration, rectification or normalization). The second approach presents different propositions in the literature and is widely used, given its ease, not requiring any information *a priori* (Hall et al., 1991; Hill & Sturm, 1991; Du et al., 2001, 2002; Furby & Campbell, 2001; Canty et al., 2004; Paolini et al., 2006; Scheidt et al., 2008). This work applies the method developed by Carvalho Júnior et al. (2006), which detects the invariant points (IP) and performs a linear regression of such points.

Structuring the input data

So as to ensure an equalitarian classification for the two times, the methods of change detection by neural networks must simultaneously process the information from the two temporal images. Usually, the multi-temporal and bi-temporal input data are structured in such a way that there is one neuron for each band of each time (Dai & Khorram, 1999; Nemmour & Chibani, 2005). Thus, the configuration of the bi-temporal input image presents as the total number of bands the summation of the two times. For example, a bi-temporal input image of TM bands, disregarding the thermal image, totals 12 neurons. Other additional information may eventually be incorporated to the training process, such as, texture information from filtering (Paola & Schowengerdt, 1995). However, in this configuration the resulting classification presents the classes of change and no change mixed, and these must be labeled by the user. Another drawback of this process is that it does not furnish the individual classification for each time, which may be of interest in the research or to assist in analysis of the results.

To avoid these inconvenient aspects, this work formulates a new configuration, in which the input data present the image from the second time as an extension of the line or column of the image of the first time. Thus, considering the two temporal images from time t_1 $(X^{\uparrow}(t_{\downarrow}1))$ and time t_2 $(X^{\uparrow}(t_{\downarrow}2))$ with the same number of lines (l) and columns (c), the input image Z_{PxQ} $(P = 2l$ and $Q = c)$ is described by the following expression:

$$Z_{PxQ} = \begin{bmatrix} X^{t_1} \\ X^{t_2} \end{bmatrix} \quad (4)$$

This procedure defines as the number of input neurons the same number of bands present at just one time. This configuration allows standardization of the parameters that describe the common classes as well as to detect any classes that may exist on just one of the dates. After the joint classification of the temporal images, these are compared by cross tabulation, to obtain the classes of change and no change.

System for detecting changes in images using SOFM

The fundamental stages of a process of classification of images using SOFM necessarily goes through the stages of training the SOFM and then classification of the image, using the map generated in the training stage. The training stage, in its turn, consists of the following steps: (1) selection of the training set made up of pixels (multi-spectral); (2) definition of the training parameter values; initial learning rate, ($\alpha(0)$); initial size of the neighborhood ($N_c(0)$); decrease rate of $\alpha(0)$; decrease rate of $N_c(0)$; and (3) application of the training algorithm.

Once trained, the SOFM neuron map can be used in the phase of image classification. In this process, each pixel (spectrum) of the image is related to one of the neurons (Eq. 3) having as a final result a classified image with the same dimensions of line and column as the input image.

This work proposes a system of detection of changes of the syn-classification type using the SOFM. Selection of the geo-positioned samples considers the two times (images *Time 1* and *Time 2*), forming just one training set (TS), so that the trained map reflects concomitant characteristics from the two times (Fig. 4).

The trained map makes feasible the process of classification that generates two classified images (one map for each time). The classification algorithm correlates each pixel (spectrum) of the input image with one of the neurons of the Kohonen Map, denominated "best matching unit" (BMU). Equation 2 is used in each pixel $e(t)$ of the input image to select its respective classifying neuron $m_c(t)$. Lastly, detection of the temporal changes is performed analyzing the transitions between the two maps of classes generated. The changes are represented by a third map of classes (resulting from the cross tabulation) which contains one class for each type of transition occurring between the maps of time 1 and time 2 (Fig. 5).

Assessment of accuracy

To assess the accuracy of the method proposed, the detection of change obtained by the SOFM is compared with that obtained by visual interpretation supported by field work. This analysis considers the classes of change and no change between the two methods. The Kappa and Overall coefficients are calculated, so as to establish statistical estimates of coincidence (Jensen, 1986; Congalton & Green, 1999).

RESULT

Use of the SOFM classifier for temporal images

Classification of the study area by the SOFM method tested different combinations referring to the initial parameters. Among the principal factors considered, the height and width of the Kohonen layer were the best,since they established the maximum number of classes. For the initial estimate of the Kohonen network, the total number of classes present on both dates was considered, where the existence of one same class at both times was computed just once. As the test area presented few classes a geometrical dimension (2×2) of the Kohonen map was used.

In the program prepared, definition of the sampling interval (sampling option), on both axis of lines and columns is done by the user. This study made use of images with dimensions of 400 lines by 400 columns; a sampling interval of 5 lines and 5 columns proved to be suitable to avoid redundancy and minimize processing time.

To avoid premature convergences, in which case the trained map does not reflect the classes representing the input images, the learning rate and the neighborhood radius were started with high values, so as to be smoothly reduced during the training, as suggested by Kohonen (1999). Both parameters (rates of learning and neighborhood) displayed an exponential decrease during the training process (Fig. 6a,b). Adjustment of the classification to the training set was verified by the proximity of its weights to the respective training samples. The same metric for selection of the winning neurons (Eq. 2) was used to calculate the average adjustment of the SOFM. The chart in Figure 6c demonstrates one case of these values throughout the cycles of training based on a SOFM, demonstrating the system's trend of adjustment.

The detections of changes made use of the following training parameters for the SOFM: initial learning rate of 0.98; initial geometry of the neighborhood equal to the smallest dimension of the map, decrease of the learning rate of 0.05 (5%); decrease of the neighborhood radius of 0.05 (5%) and maximum quantity of training cycles of 1000.

The image from 1984 demonstrated a highly-preserved area containing an expressive area of natural vegetation, represented by class 3 (Fig. 7). In just one of the restricted areas was there a predominance of exposed soil (described as class 1). The classified image from 2006 demonstrated a significant change of landscape, where there appear extensive classes linked to crops with different rates of growth (described by the class 1, 2 and 4).

Besides the images classified for each time the program also furnished the image of the Kohonen network. This image was characterized by having the number of lines and columns according to the geometry of the network defined by the user (height and width), plus the same number of bands as the input image. In this image each pixel has a vector of specific weights referring to each spectral band that characterizes a determined class. In the

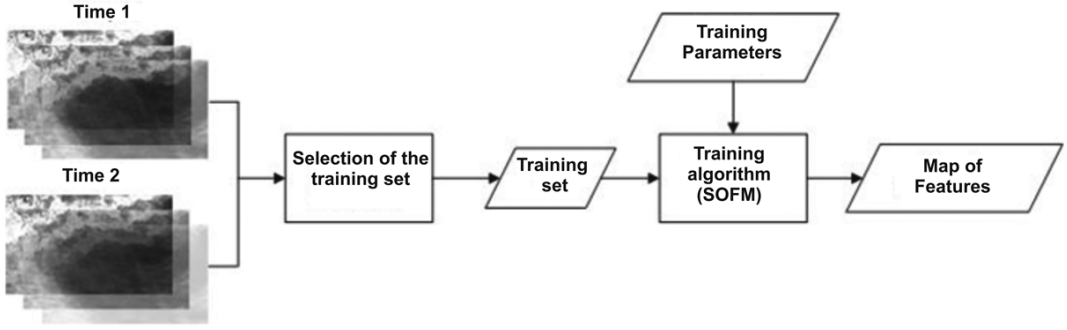

Figure 4 – Training with bi-temporal samples.

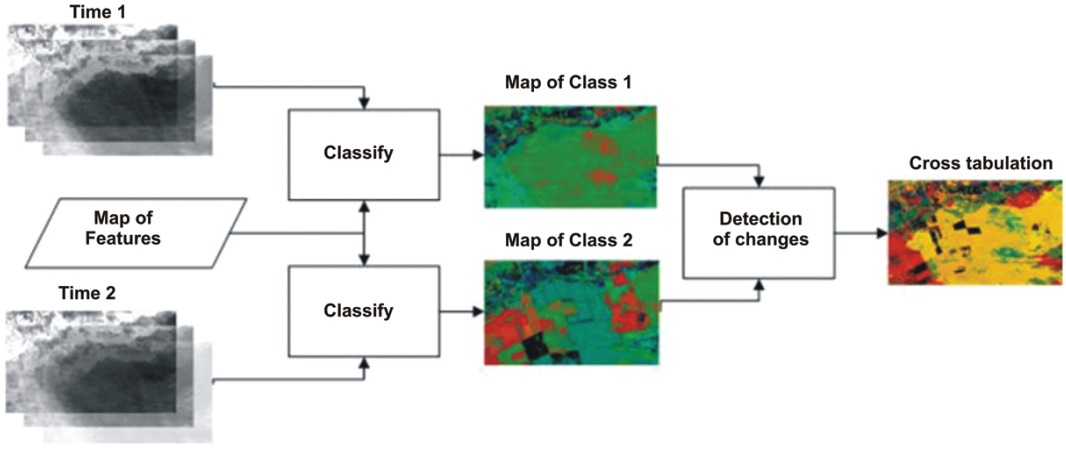

Figure 5 – Syn-classification and detection of temporal changes.

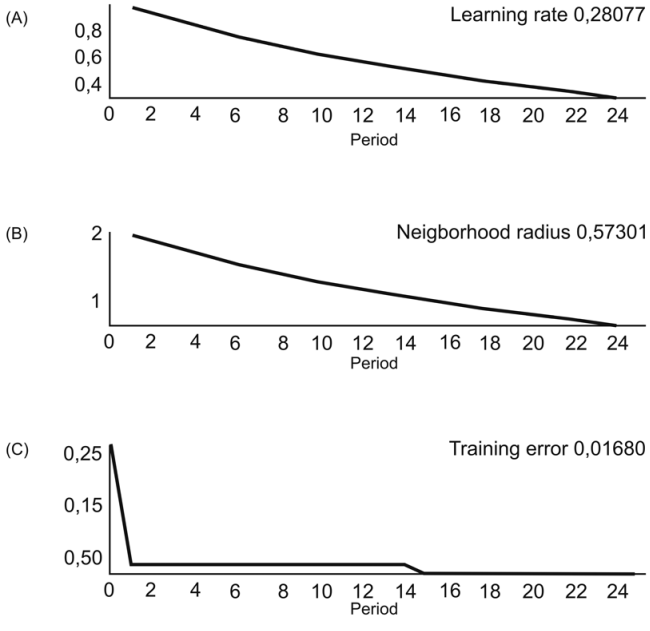

Figure 6 – (a) curve of the learning rate; (b) curve of the neighborhood radius, and (c) curve of the training error.

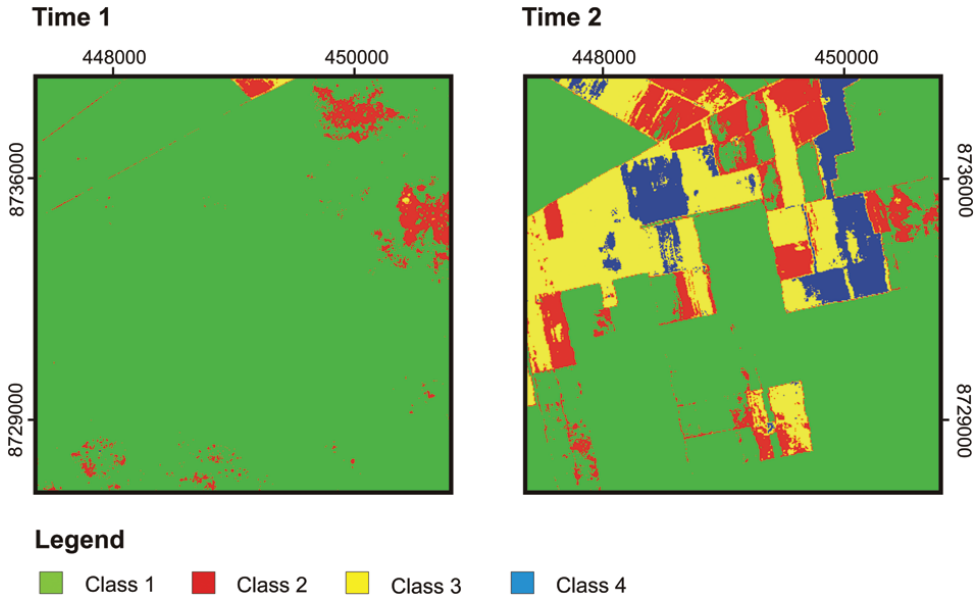

Figure 7 – Classification of bi-temporal images using the SOFM method, considering a geometry of 2×2 for the Kohonen map.

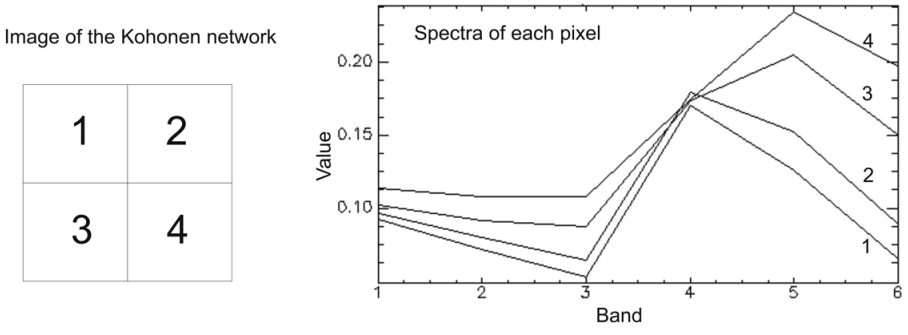

Figure 8 – Image of the Kohonen network (2×2) containing four pixels, containing vectors of weights that report the spectra of a continuous transition from photo-synthetically active vegetation to bare soil.

chart of Figure 8 the spectra of weights obtained for the image in question represented a continual spectral transition from photo-synthetically active vegetation (PAV) (spectrum 1) to exposed soil (spectrum 4). Therefore, the Kohonen network permitted evidencing the different targets present on the scene as components of spectral mixtures.

The comparison of the two images classified at the two times by cross tabulation generated a new image related to the areas of change consisting of 8 classes and the areas of no change with 3 classes (Fig. 9). In this image it was possible to verify the process of change that took place, assessing the different modifying actions present in the environment. As the classes are ordered with graded losses of PAV, it was noted that change class 1:4 represented the greatest alteration, going from a situation of vegetation cover to exposed soil. The classes in which the first index proved to be lower than the second (2:1; 3:1 and 3:2) were the areas with higher PAV, meaning a recovery of the ambient.

Result of assessment of accuracy

In the assessment of accuracy the categories related to change and no change were used, these obtained by simple grouping of the respective classes. The comparison of detection of change by the SOFM method and by visual interpretation displayed significant values of the Kappa coefficient of 0.875 and Overall of 94.0%.

The areas with changes not detected by the SOFM method proved to be concentrated at two locations (Fig. 10): (a) trails and roads, and (b) areas of conversion of the Cerrado grasslands into cultivation, where both are characterized by the spectral behav-

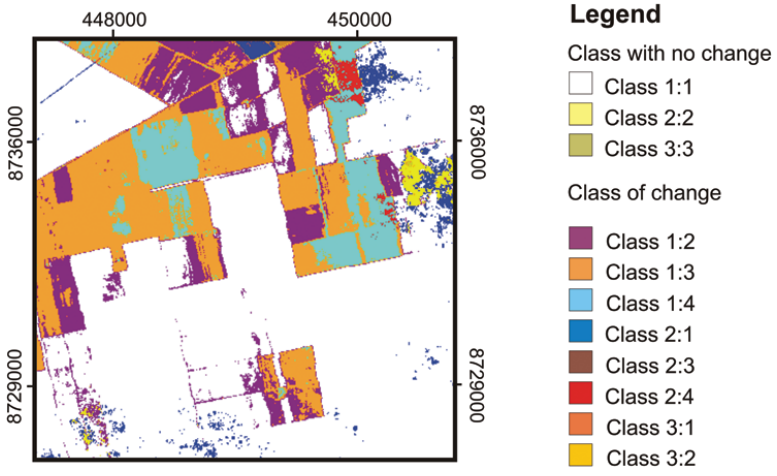

Figure 9 – Detection of changes based on the cross tabulation of images classified by the SOFM method.

ior of photo-synthetically active vegetation. The transformation of the interpreted vectors of roads into an image makes it hard to maintain a perfect adjustment with that obtained directly by visual classification, in both their continuity and width, causing errors. Thus, in this work, roads were not considered in the visual interpretation, always being computed as an error of the method proposed. A second error occurring consisted of areas that continued to have photo-synthetically active vegetation, in spite of different origins, one related to cultivation and the other to natural vegetation. This error proved hard to detect, due to the spectral similarity of the two situations, as was already evidenced in other methods of automated change detection (Carvalho Júnior et al., 2011).

The areas where the proposed method indicated change not identified in the visual interpretation occurred principally in areas of vegetation fire scars and once again on roads (Fig. 11). The scars from vegetation fires, in spite of being changes, were not classified by visual interpretation as they display non-continuous behavior and are included in an area of natural vegetation. Therefore, the greater sensitivity of the method proposed in the detection of roads and scars from vegetation fires ends up being a source of errors that must be minimized in the analysis. Thus, the Kappa and Overall values obtained display underestimated values due to roads and fire scars that were disregarded in the visual interpretation.

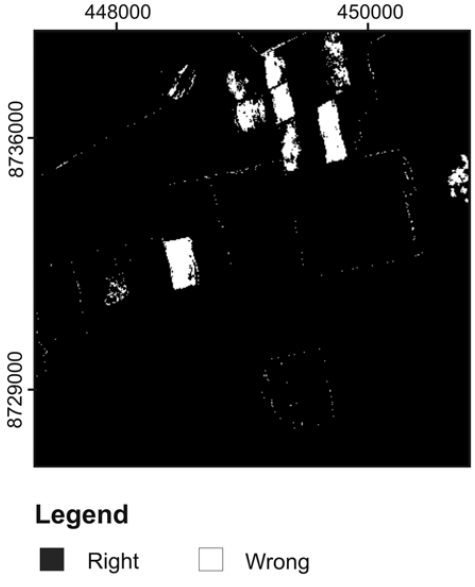

Figure 10 – Image of the areas with changes present in the visual interpretation, not detected by the method proposed.

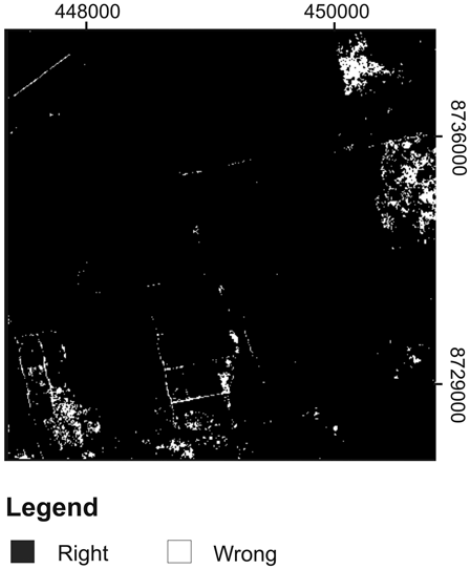

Figure 11 – Image of the areas where the method proposed indicated changes not occurring in the visual interpretation.

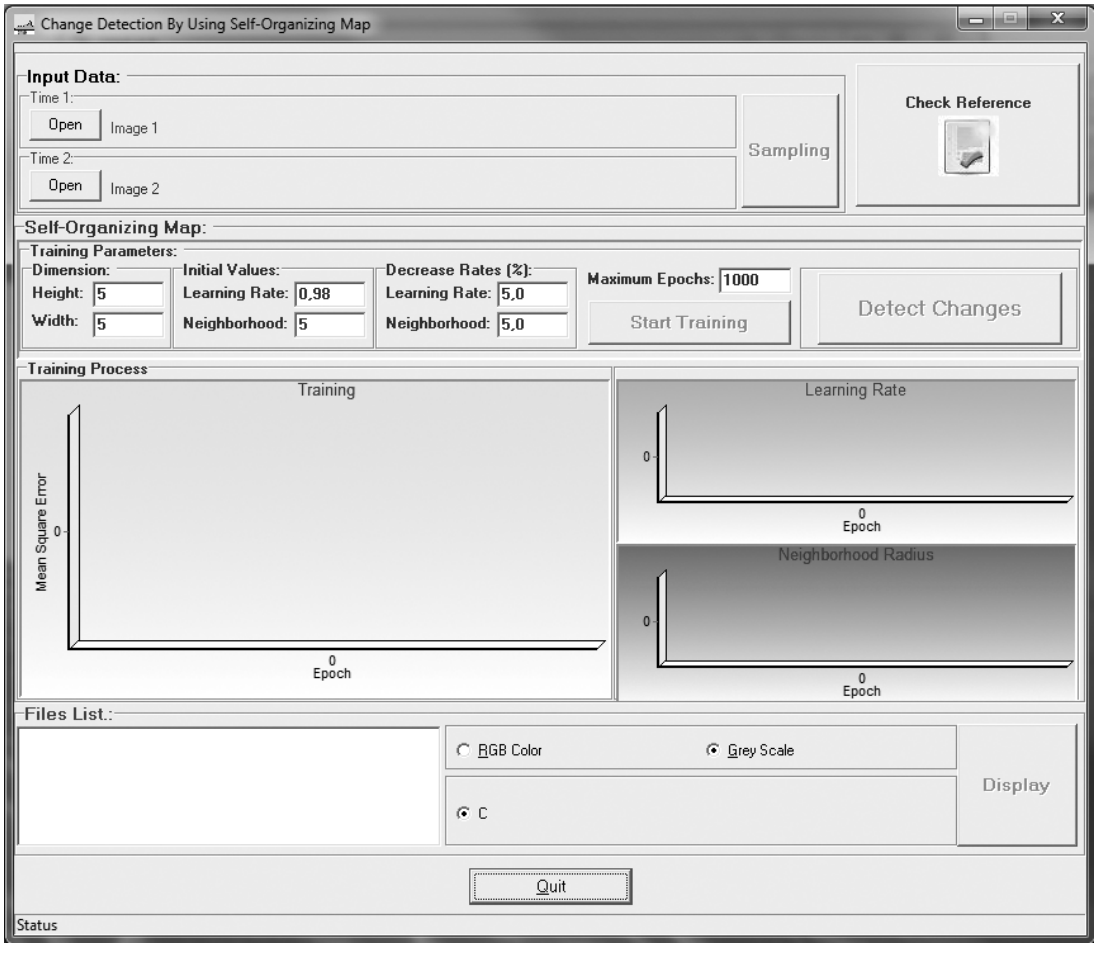

Figure 12 – Principal display of the program of change detection using SOFM.

Program of change detection using SOFM

The method proposed is made available in the form of a program developed in C++ language. The functions of the program are organized in an interface consisting of the following components: inputting the images, configuration of the parameters of the SOFM classifier and display of the resulting images (Fig. 12).

Two temporal images with the same dimensions and co-recorded are required as input data. The program reads the raster files in the formats BSO (Band Sequential Format) and BIP (Band Interleaved by Pixel Format) in which each image must be accompanied by a header file containing the following information on the image: number of lines, columns and bands, format code of the images (BIP or BSO) and type of data (byte, whole, floating point, 64-bit whole).

The training stage (option Start Training) requires definition of the training set (option Sampling) and definition of the training parameters discussed in section 2.3 (option Training Parameters). The option Start Training starts the SOFM training algorithm. At each cycle of presenting the training set, three accompanying graphics are updated: graphic of the mean squared error of classification of the training set, graphic of decrease of the learning rate, and graphic of decrease of the radius of the neighborhood function. At the end of the training, the final values of the mean squared error of classification of the training set, the learning rate and the neighborhood radius are shown as subtitles of the graphics.

The option Detect Change starts the process of classifying the Time 1 and Time 2 images with the subsequent detection of changes. At the end, the following result images are generated in the File list (Fig. 12): (a) Map of classes of images from Time 1, (b) Map of classes of images from Time 2, (c) Map of classes of temporal changes (Change image).

As exemplified in Figure 13, all the resulting images may be displayed in the form of levels of gray and colored composition,

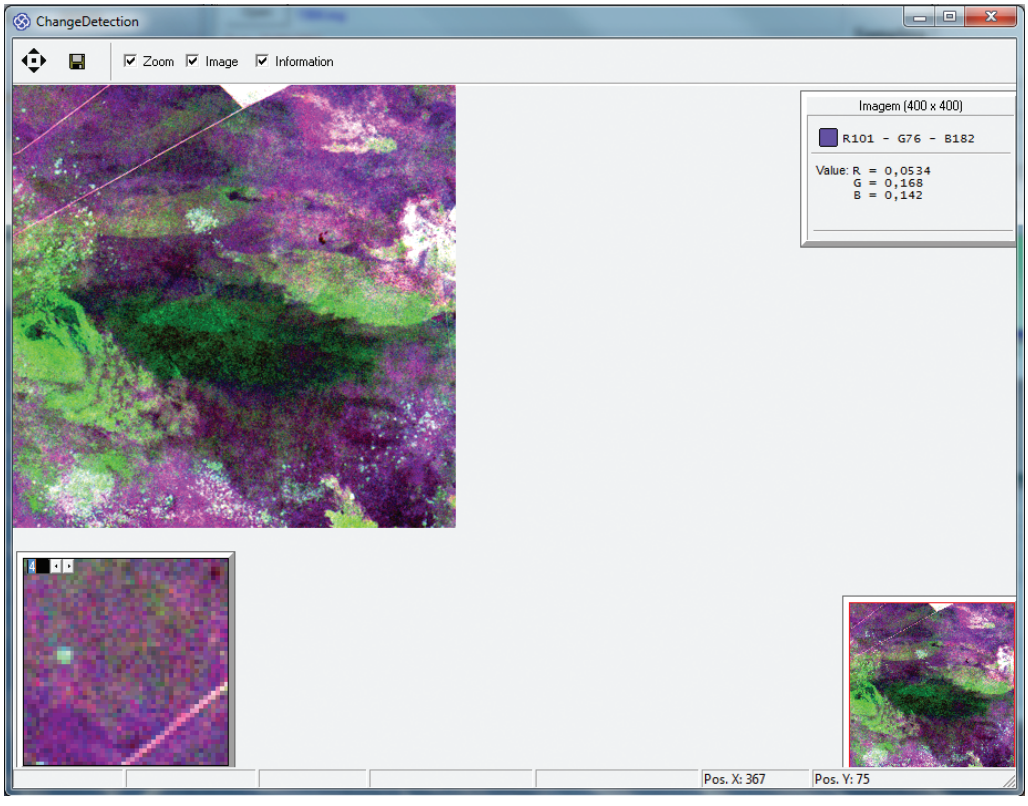

Figure 13 – Image display interface.

based on the list of files (option Files List). The display interface presents basic functions such as zoom and pixel reader. The images may be read by other programs such as ENVI.

CONCLUSION

This work devises a semi-automatic method of change detection using an unsupervised classifier (the artificial neural network SOFM). The methodological procedure demonstrated here makes feasible research proposing the temporal monitoring of transformations on the earth's surface. As an advantage, the method presented the following factors: (a) unsupervised classification, not requiring *a priori* samples of the classes; (b) the number of classes present depends on the interest of the user; (c) generation of classified images for each time and the criteria adopted in selection of the classes adopt concomitant bi-temporal information. Moreover, the method adopts a procedure of differentiated data input where samples are collected in the images related to the two times. This procedure allows detection of the direction of the changes occurring, defining the areas that have had changes and no changes. In the case of adopting all the images of discrete variables in the Kohonen network, the different classes are identified, but the direction of the change is not obtained automatically.

Comparison of classification by the method proposed with visual interpretation demonstrates significant values of Overall and Kappa coefficient. In part, the source of errors arises from the visual interpretation map, which reveals difficulty in comparing linear features such as roads and dispersed features and non-continuous features such as vegetation fire scars. The most significant error are the areas that correspond to change, yet maintain the same spectral behavior in relation to the areas of the grasslands converted to croplands, since thesepossess the same spectrum of photo-synthetically active vegetation.

ACKNOWLEDGMENTS

The authors wish to thank the support received during the development of this work from the following institutions: Coordenação de Aperfeiçoamento de Pessoal de Nível Superior (CAPES) for financing the post-doctorate scholarship of Professor Nilton Correia da Silva and Conselho Nacional de Desenvolvimento Científico e Tecnológico (CNPq) for financing the research productivity scholarships of Professors Osmar Abílio de Carvalho Júnior, Renato Fontes Guimarães and Roberto Arnaldo Trancoso Gomes.

REFERENCES

BYRNE GF, CRAPPER PF & MAYO KK. 1980. Monitoring land cover change by principal component analysis of multitemporal Landsat data. Remote Sensing of Environment, 10: 175–184.

CAKIR HI, KHORRAM S & NELSON SAC. 2006. Correspondence analysis for detecting land cover change. Remote Sensing of Environment, 102(3-4): 306–317.

CANTY MJ, NIELSEN AA & SCHMIDT M. 2004. Automatic radiometric normalization of multitemporal satellite imagery. Remote Sensing of Environment, 91(3-4): 441–451.

CARPENTER GA, GJAJA MN, GOPAL S & WOODCOCK CE. 1997. ART neural networks for remote sensing: vegetation classification from Landsat TM and terrain data. IEEE Transactions on Geoscience and Remote Sensing, 35(2): 308–325.

CARPENTER GA, GOPAL S, MACOMBER S, MARTENS S, WOODCOCK CE & FRANKLIN J. 1999. A neural network method for efficient vegetation mapping. Remote Sensing of Environment, 70(3): 326–338.

CARVALHO JÚNIOR OA, GUIMARÃES RF, GOMES RAT, CARVALHO APF & SILVA NC. 2006. Normalization of multi-temporal images using a new change detection method based on the spectral classifier. In: IEEE International Geoscience & Remote Sensing Symposium, Denver, Colorado. Proceedings... Piscataway, NJ: IEEE, p. 771–774.

CARVALHO JÚNIOR OA, GUIMARÃES RF, GILLESPIE AR, SILVA NC & GOMES RAT. 2011. A New Approach to Change Vector Analysis Using Distance and Similarity Measures. Remote Sensing, 3: 2473–2493.

CONGALTON R & GREEN, K. 1999. Assessing the Accuracy of Remotely Sensed Data: Principles and Practices. Boca Raton, FL, USA: CRC/Lewis Press. 137 p.

COPPIN P, NACKAERTS K, QUEEN L & BREWER K. 2001. Operational monitoring of green biomass change for forest management. Photogrammetric Engineering & Remote Sensing, 67: 603–611.

COPPIN PR, JONCKHEERE I, NACKAERTS K, MUYS B & LAMBIN E. 2004. Digital change detection methods in ecosystem monitoring: a review. International Journal of Remote Sensing, 25(9): 1565–1596.

DAI X & KHORRAM S. 1998. The effects of image misregistration on the accuracy of remotely sensed change detection. IEEE Transactions on Geoscience and Remote Sensing, 36(5): 1566–1577.

DAI XL & KHORRAM S. 1999. Remotely sensed change detection based on artificial neural networks. Photogrammetric Engineering & Remote Sensing, 65(10): 1187–1194.

DU Y, CIHLAR J, BEAUBIEN J & LATIFOVIC R. 2001. Radiometric normalization, compositing, and quality control for satellite high resolution image mosaics over large areas. Transactions on Geoscience & Remote Sensing, 39(3): 623–634.

DU Y, TEILLET PM & CIHLAR J. 2002. Radiometric normalization of multitemporal high-resolution satellite images with quality control for land cover change detection. Remote Sensing of Environment, 82: 123–134.

DYMOND CC, MLADENOFF DJ & RADELOFF VC. 2002. Phenological differences in Tasseled Cap indices improve deciduous forest classification. Remote Sensing of Environment, 80: 460–472.

FRANKLIN SE, LAVIGNE MB, WULDER MA & McCAFFREY TM. 2002. Large-area forest structure change detection: An example. Canadian Journal of Remote Sensing, 28(4): 588–592.

FRANKLIN SE, MOSKAL LM, LAVIGNE MB & PUGH K. 2000. Interpretation and classification of partially harvested forest stands in the Fundy model forest using multitemporal Landsat TM digital data. Canadian Journal of Remote Sensing, 26(4): 318–333.

FRANKLIN SE, WULDER MA, SKAKUN RS & CARROLL AL. 2003. Mountain pine beetle red-attack forest damage classification using stratified Landsat TM data in British Columbia, Canada. Photogrammetric Engineering & Remote Sensing, 69: 283–288.

FUNG T & LE DREW E. 1987. Application of principal components analysis to change detection. Photogrammetric Engineering & Remote Sensing, 53: 1649–1658.

FURBY SL & CAMPBELL NA. 2001. Calibrating images from different dates to 'like-value' digital counts. Remote Sensing of Environment, 77: 186–196.

GONG P, LEDREW EF & MILLER JR. 1992. Registration-noise reduction difference images for change detection. International Journal of Remote Sensing, 13: 773–779.

GOPAL S & WOODCOCK CE. 1996. Remote sensing of forest change using artificial neural networks. IEEE Transactions on Geoscience and Remote Sensing, 34(2): 398–404.

GOPAL S, WOODCOCK CE & STRAHLER AH. 1999. Fuzzy neural network classification of global land cover from a 1-degree AVHRR data set. Remote Sensing of Environment, 67: 230–243.

GROSSBERG S. 1976. Adaptive pattern classification and universal recoding, II. Feedback, expectation, olfaction, and illusions. Biological Cybernetics, 23: 187–202.

HALL FG, STREBEL DE, NICKESON JE & GOETZ SJ. 1991. Radiometric rectification: Toward a common radiometric response among multidate, multisensor images. Remote Sensing of Environment, 35: 11–27.

HALL O & HAY GJ. 2003. A Multiscale Object-Specific Approach to Digital Change Detection. International Journal of Applied Earth Observation and Geoinformation, 4: 311–327.

HAYES DJ & SADER SA. 2001. Comparison of change-detection techniques for monitoring tropical forest clearing and vegetation regrowth in a time series. Photogrammetric Engineering & Remote Sensing, 67(9): 1067–1075.

HECHT-NIELSEN R. 1990. Neurocomputing. Addison-Wesley Publishing Company, Reading, 433 p.

HILL J & STURM B. 1991. Radiometric correction of multitemporal thematic mapper data for use in agricultural landcover classification and vegetation monitoring. International Journal of Remote Sensing, 12: 1471–1491.

HOWARTH PJ & MICKWARE GM. 1981. Procedures for change detection using Landsat digital data. International of Remote Sensing, 2: 277–279.

JENSEN JR. 1986. Introductory Digital Image Processing. Englewood Cliffs, New Jersey, USA: Prentice-Hall. 379 p.

JENSEN JR, COWEN DJ, NARUMALANI S, ALTHAUSEN JD & WEATHERBEE O. 1993. An evaluation of Coastwatch change detection protocol in South Carolina. Photogrammetric Engineering & Remote Sensing, 59(4): 519–525.

JIANWEN M & BAGAN H. 2005. Land-use classification using ASTER data and self-organized neutral networks. International Journal of Applied Earth Observation and Geoinformation, 7: 183–188.

JIN S & SADER SA. 2005. Comparison of time series tasseled cap wetness and the normalized difference moisture index in detecting forest disturbances. Remote Sensing of Environment, 94: 364–372.

KAIMOWITZ D & SMITH J. 2001. Soybean technology and the loss of natural vegetation in Brazil and Bolivia. In: ANGELSEN A & KAIMOWITZ D (Eds.). Agricultural Technologies and Tropical Deforestation, CABI Publishing, New York, pp. 195–211.

KOHONEN T. 1982. Self-Organized formation of topologically correct feature maps. Biological Cybernetics, 43: 59–69.

KOHONEN T. 1988. Statistical pattern recognition with neural networks: benchmarking studies. In: IEEE International Conference on Neural Networks, San Diego, CA. Proceedings... IEEE p. 61–68.

KOHONEN T. 1990. The self-organizing map. Proceedings of the IEEE, 78(9): 1464–1480.

KOHONEN T & MÄKISARA K. 1989. The self-organizing feature maps. Physica Scripta, 39: 168.

LAMBIN EF. 1999. Monitoring Forest Degradation in Tropical Regions by Remote Sensing: Some Methodological Issues. Global Ecology and Biogeography, 8(3/4): 191–198.

LU D, MAUSEL P, BRONDÍZIO E & MORAN E. 2003. Change detection techniques. International Journal of Remote Sensing, 25(12): 2365–2407.

MENKE AB, CARVALHO JÚNIOR OA, GOMES, RAT, MARTINS, ES & OLIVEIRA SN. 2009. Análise das mudanças do uso agrícola da terra a partir de dados de sensoriamento remoto multitemporal no município de Luis Eduardo Magalhães (Bahia – Brasil). Sociedade & Natureza, 21(3): 315–326.

NEMMOUR H & CHIBANI Y. 2005. Neural network combination by fuzzy integral for robust change detection in remotely sensed imagery. 2005. EURASIP Journal on Applied Signal Processing, 14: 2187–2195.

PAOLA JD & SCHOWENGERDT RA. 1995. A detailed comparison of backpropagation neural network and maximum-likelihood classifiers for urban land use classification. IEEE Transactions on Geoscience and Remote Sensing, 33(4): 981–996.

PAOLINI L, GRINGS F, SOBRINO JA, JIMENEZ MUNOZ JC & KARSZENBAUM H. 2006. Radiometric correction effects in Landsat multi-date/multi-sensor change detection studies. International Journal of Remote Sensing, 27(4): 685–704.

PAPA JP, FALCAO AX, DE FREITAS GM & DE AVILA A. 2010. Robust Pruning of Training Patterns for Optimum-Path Forest Classification Applied to Satellite-Based Rainfall Occurrence Estimation. Geoscience and Remote Sensing Letters, IEEE, 7(2): 396–400.

PONZONI FJ & SHIMABUKURO YE. 2007. Sensoriamento Remoto no Estudo da Vegetação. Ed. Parêntese. São José dos Campos, São Paulo. 127 p.

RESEARCH SYSTEMS. 2001. ENVI User's Guide. Boulder, CO: Research Systems, Inc. 614 p.

SADER SA, HAYES DJ, HEPINSTALL, JA, COAN M & SOZA C. 2001. Forest change monitoring of a remote biosphere reserve. International Journal of Remote Sensing, 22(10): 1937–1950.

SCHEIDT S, RAMSEY M & LANCASTER N. 2008. Radiometric normalization and image mosaic generation of ASTER thermal infrared data: An application to extensive sand sheets and dune fields. Remote Sensing of Environment, 112: 920–933.

SILVA NC. 2003. Síntese Genética de Redes Neurais Artificiais. Ph.D. Thesis in Geoscience – Instituto de Geociências, Universidade de Brasília, Brasília. 123 p.

SINGH A. 1989. Digital change detection techniques using remotely-sensed data. International Journal of Remote Sensing, 10: 989–1003.

SKAKUN RS, WULDER MA & FRANKLIN SE. 2003. Sensitivity of the thematic mapper enhanced wetness difference index to detect mountain pine beetle red-attack damage. Remote Sensing of Environment, 86: 433–443.

SMITH J, WINOGRAD M, GALLOPIN G & PACHICO D. 1998. Dynamics of the agricultural frontier in the Amazon and savannas of Brazil: analyzing the impact of policy and technology. Environmental Modeling and Assessment, 3: 31–46.

SOARES VP & HOFFER RM. 1994. Eucalyptus forest change classification using multi-data Landsat TM data. Proceedings, International Society of Optical Engineering (SPIE), 2314: 281–291.

TSYPKIN YAZ. 1973. Foundations of the Theory of Learning Systems. Academic Press, New York, 205 p.

WEISMILLER RA, KRISTOF SJ, SCHOLZ DK, ANUTA PE & MOMIN SA. 1977. Change detection in coastal zone environments. Photogrammetric Engineering & Remote Sensing, 43: 1533–1539.

WILLIAMS RJ. 1985. Feature discovery through error correction learning. ICS Report 8501, Inst. of Cognitive Science, University of California, San Diego. 45 p.

WILSON EH & SADER SA. 2002. Detection of forest harvest type using multiple dates of Landsat TM imagery. Remote Sensing of Environment, 80: 385–396.

YUAN D & ELVIDGE C. 1998. NALC Land Cover Change Detection Pilot Study: Washington D.C. Area Experiments. Remote Sensing of Environment, 66: 66–178.

YUAN F, SAWAYA KE, LOEFFELHOLZ B & BAUER ME. 2005. Land cover classification and change analysis of the Twin Cities (Minnesota) metropolitan area by multitemporal. Landsat remote sensing. Remote Sensing of Environment, 98(2): 317–328.

NOTES ABOUT THE AUTHORS

Nilton Correia da Silva. Graduate in computing from Universidade Estadual de Goiás (1994). Master's Degree in Computing Science from the Department of Computing Science, Universidade de Brasília (1999). Doctorate in Data Processing and Environmental Analysis from the Institute of Geosciences, Universidade de Brasília (2003). Post-doctorate internship in Temporal Analysis in Remote Sensing Images at the Universities of Brasília (UnB) and Washington (UW-Seattle) (2011). Currently doing Post-doctorate work on recognition of patterns in remote sensing images; professor/researcher of the Faculdade de Engenharias do Gama, Universidade de Brasília. Experienced in Computer Sciences, with emphasis on the application of intelligent agents in digital image processing, mainly active in the research and development of specialist systems for the treatment of remote sensing images using intelligent agents, evolutionary computing and mathematical methods.

Osmar Abílio de Carvalho Júnior. Geologist graduated at Universidade de Brasília in 1990. Master and doctorate degrees in mineral prospection from Universidade de Brasília in 1995 and 2000, respectively. Worked as a Researcher at Instituto Nacional de Pesquisas Espaciais (INPE) from 2002 to 2004. Currently is a professor at Universidade de Brasília, CNPq 1B research fellowship, performing research in digital processing of multi-spectral and hyper-spectral images.

Antonio Nuno de Castro Santa Rosa. Graduate in Mathematics from Universidade da Amazônia (1984). Master's Degree in Geophysics from Universidade Federal do Pará (1989). Doctorate in Geophysics from Universidade Federal do Pará (1996) and Post-doctorate in Applied Computing from Instituto Nacional de Pesquisas Espaciais (2001). Associate Professor II at Universidade de Brasília. Group Leader of Research in Automatic Image Processing and Interpretation. Researcher in the GPDS Research Group in Forensic Computer Science: Facial Recognition. Member of the Editorial Boardof the Journal of Forensic Computer Science.

Renato Fontes Guimarães. Graduate in Cartographic Engineering from Universidade do Estado do Rio de Janeiro (1987), master's degree in Geophysics from the Observatório Nacional (1991) and doctor in Geology from Universidade Federal do Rio de Janeiro (2000). Currently assistant professor at Universidade de Brasília, holding a scholarship for productivity and research from CNPq IC. Reviwer of Revista Brasileira de Geociências, Revista Brasileira de Cartografia, International Journal of Remote Sensing (Online), Risk Analysis and Espaço e Geografia (UnB). Active member of the Editorial Boardof Revista Brasileira de Cartografia and Espaco e Geografia (UnB). Experience Geosciences, with emphasis on Physical Geography. Main research themes: Mathematical Modeling, landslides, SHALSTAB Model, Digital Terrain Model.

Roberto Arnaldo Trancoso Gomes. Graduate in Geography from Universidade Federal do Rio de Janeiro (1999). Master's degree in Geography from Universidade Federal do Rio de Janeiro (2002) and a doctorate in Geography from Universidade Federal do Rio de Janeiro (2006). Currently assistant professor at Universidade de Brasília, Geography Department, CNPq research fellowship. Experience in Geosciences, with emphasis on Physical Geography. Main research themes: Mass Flow Forecasting Models. Landslides. Geographical Information Systems and cartography.